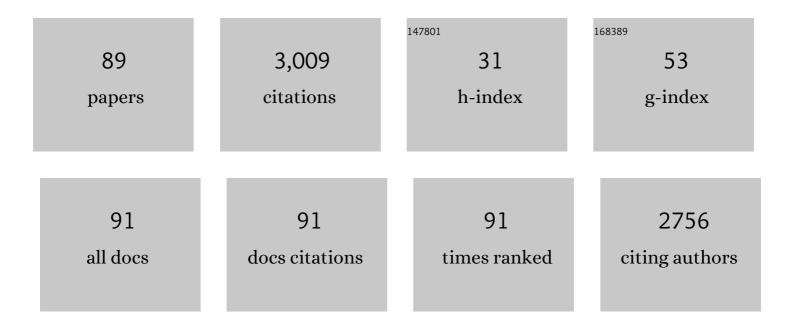
List of Publications by Year in descending order

Source: https://exaly.com/author-pdf/6225911/publications.pdf Version: 2024-02-01



#	Article	IF	CITATIONS
1	Reducing electron beam damage through alternative STEM scanning strategies, Part I: Experimental findings. Ultramicroscopy, 2022, 232, 113398.	1.9	22
2	Event driven 4D STEM acquisition with a Timepix3 detector: Microsecond dwell time and faster scans for high precision and low dose applications. Ultramicroscopy, 2022, 233, 113423.	1.9	36
3	Reducing electron beam damage through alternative STEM scanning strategies, Part II: Attempt towards an empirical model describing the damage process. Ultramicroscopy, 2022, 240, 113568.	1.9	4
4	Fast versus conventional HAADF-STEM tomography of nanoparticles: advantages and challenges. Ultramicroscopy, 2021, 221, 113191.	1.9	17
5	Three-dimensional atomic structure of supported Au nanoparticles at high temperature. Nanoscale, 2021, 13, 1770-1776.	5.6	13
6	Optimizing Experimental Conditions for Accurate Quantitative Energy-Dispersive X-ray Analysis of Interfaces at the Atomic Scale. Microscopy and Microanalysis, 2021, 27, 528-542.	0.4	6
7	Reaching for atomic-scale quantitative energy dispersive X-ray spectroscopy. Microscopy and Microanalysis, 2021, 27, 2602-2603.	0.4	0
8	Novel class of nanostructured metallic glass films with superior and tunable mechanical properties. Acta Materialia, 2021, 213, 116955.	7.9	32
9	Fast electron low dose tomography for beam sensitive materials. Microscopy and Microanalysis, 2021, 27, 2116-2118.	0.4	2
10	Coincidence Detection of EELS and EDX Spectral Events in the Electron Microscope. Applied Sciences (Switzerland), 2021, 11, 9058.	2.5	10
11	Strain measurement in semiconductor FinFET devices using a novel moiré demodulation technique. Semiconductor Science and Technology, 2020, 35, 034002.	2.0	10
12	3D Characterization and Plasmon Mapping of Gold Nanorods Welded by Femtosecond Laser Irradiation. ACS Nano, 2020, 14, 12558-12570.	14.6	30
13	HAADF-STEM block-scanning strategy for local measurement of strain at the nanoscale. Ultramicroscopy, 2020, 219, 113099.	1.9	5
14	Single femtosecond laser pulse excitation of individual cobalt nanoparticles. Physical Review B, 2020, 102, .	3.2	1
15	Evaluation of different rectangular scan strategies for STEM imaging. Ultramicroscopy, 2020, 215, 113021.	1.9	10
16	Viability of Compressed Sensing as a Dose Reduction Strategy in STEM. Microscopy and Microanalysis, 2019, 25, 1686-1687.	0.4	3
17	Quantification of 3D Atomic Structures and Their Dynamics by Atom-Counting from an ADF STEM Image. Microscopy and Microanalysis, 2019, 25, 1808-1809.	0.4	0
18	Prospects for out-of-plane magnetic field measurements through interference of electron vortex modes in the TEM. Journal of Optics (United Kingdom), 2019, 21, 124002.	2.2	4

#	Article	IF	CITATIONS
19	Atomic-scale viscoplasticity mechanisms revealed in high ductility metallic glass films. Scientific Reports, 2019, 9, 13426.	3.3	13
20	Various Compressed Sensing Setups Evaluated Against Shannon Sampling Under Constraint of Constant Illumination. IEEE Transactions on Computational Imaging, 2019, 5, 502-514.	4.4	8
21	Electron Bessel beam diffraction for precise and accurate nanoscale strain mapping. Applied Physics Letters, 2019, 114, 243501.	3.3	20
22	Experimental Evaluation of Undersampling Schemes for Electron Tomography of Nanoparticles. Particle and Particle Systems Characterization, 2019, 36, 1900096.	2.3	13
23	Spectroscopic coincidence experiments in transmission electron microscopy. Applied Physics Letters, 2019, 114, .	3.3	19
24	Asymmetry and non-dispersivity in the Aharonov-Bohm effect. Nature Communications, 2019, 10, 1700.	12.8	10
25	Control of Knock-On Damage for 3D Atomic Scale Quantification of Nanostructures: Making Every Electron Count in Scanning Transmission Electron Microscopy. Physical Review Letters, 2019, 122, 066101.	7.8	14
26	Comparison of first moment STEM with conventional differential phase contrast and the dependence on electron dose. Ultramicroscopy, 2019, 203, 95-104.	1.9	29
27	Demonstration of a 2â€ [–] ×â€ [–] 2 programmable phase plate for electrons. Ultramicroscopy, 2018, 190, 58-65.	1.9	80
28	3D characterization of heat-induced morphological changes of Au nanostars by fast <i>in situ</i> electron tomography. Nanoscale, 2018, 10, 22792-22801.	5.6	56
29	Orthorhombic vs. hexagonal epitaxial SrIrO 3 thin films: Structural stability and related electrical transport properties. Europhysics Letters, 2018, 122, 28003.	2.0	4
30	Efficient creation of electron vortex beams for high resolution STEM imaging. Ultramicroscopy, 2017, 178, 12-19.	1.9	37
31	Probing the symmetry of the potential of localized surface plasmon resonances with phase-shaped electron beams. Nature Communications, 2017, 8, 14999.	12.8	95
32	Theory and applications of free-electron vortex states. Physics Reports, 2017, 690, 1-70.	25.6	227
33	Direct observation of enhanced magnetism in individual size- and shape-selected <mml:math xmlns:mml="http://www.w3.org/1998/Math/MathML"> <mml:mrow> <mml:mn>3 </mml:mn> <mml:mi>d transition metal nanoparticles. Physical Review B, 2017, 95, .</mml:mi></mml:mrow></mml:math 	i> ⊲/ഛ ml:r	nrœ4>
34	Measurement of atomic electric fields and charge densities from average momentum transfers using scanning transmission electron microscopy. Ultramicroscopy, 2017, 178, 62-80.	1.9	106
35	Locating light and heavy atomic column positions with picometer precision using ISTEM. Ultramicroscopy, 2017, 172, 75-81.	1.9	9
36	Determining oxygen relaxations at an interface: A comparative study between transmission electron microscopy techniques. Ultramicroscopy, 2017, 181, 178-190.	1.9	36

#	Article	IF	CITATIONS
37	Measurement of Atomic Electric Fields by Scanning Transmission Electron Microscopy (STEM) Employing Ultrafast Detectors. Microscopy and Microanalysis, 2016, 22, 484-485.	0.4	1
38	Development of a fast electromagnetic beam blanker for compressed sensing in scanning transmission electron microscopy. Applied Physics Letters, 2016, 108, .	3.3	51
39	Symmetry-constrained electron vortex propagation. Physical Review A, 2016, 93, .	2.5	9
40	Strain mapping of semiconductor specimens with nm-scale resolution in a transmission electron microscope. Micron, 2016, 80, 145-165.	2.2	104
41	Focused electron beam induced deposition as a tool to create electron vortices. Micron, 2016, 80, 34-38.	2.2	23
42	Electron Microscopy of Probability Currents at Atomic Resolution. Physical Review Letters, 2015, 115, 176101.	7.8	17
43	Quantitative annular dark field scanning transmission electron microscopy for nanoparticle atom-counting: What are the limits?. Journal of Physics: Conference Series, 2015, 644, 012034.	0.4	0
44	Quantitative STEM normalisation: The importance of the electron flux. Ultramicroscopy, 2015, 159, 46-58.	1.9	26
45	Prospects for versatile phase manipulation in the TEM: Beyond aberration correction. Ultramicroscopy, 2015, 151, 85-93.	1.9	23
46	Dose limited reliability of quantitative annular dark field scanning transmission electron microscopy for nano-particle atom-counting. Ultramicroscopy, 2015, 151, 56-61.	1.9	47
47	Phase problem in the B-site ordering of La ₂ CoMnO ₆ : impact on structure and magnetism. Nanoscale, 2015, 7, 9835-9843.	5.6	40
48	Using electron vortex beams to determine chirality of crystals in transmission electron microscopy. Physical Review B, 2015, 91, .	3.2	62
49	3D Magnetic Induction Maps of Nanoscale Materials Revealed by Electron Holographic Tomography. Chemistry of Materials, 2015, 27, 6771-6778.	6.7	64
50	Atomic electric fields revealed by a quantum mechanical approach to electron picodiffraction. Nature Communications, 2014, 5, 5653.	12.8	232
51	Measuring the orbital angular momentum of electron beams. Physical Review A, 2014, 89, .	2.5	42
52	Quantitative measurement of orbital angular momentum in electron microscopy. Physical Review A, 2014, 89, .	2.5	26
53	Atomistic structure of Cu-containing β″ precipitates in an Al–Mg–Si–Cu alloy. Scripta Materialia, 2014, 75, 86-89.	5.2	63
54	Magnetic monopole field exposed by electrons. Nature Physics, 2014, 10, 26-29.	16.7	141

#	Article	IF	CITATIONS
55	Shaping electron beams for the generation of innovative measurements in the (S)TEM. Comptes Rendus Physique, 2014, 15, 190-199.	0.9	24
56	Getting the Best from an Imperfect Detector - an Alternative Normalisation Procedure for Quantitative HAADF STEM. Microscopy and Microanalysis, 2014, 20, 126-127.	0.4	1
57	Strain measurement at the nanoscale: Comparison between convergent beam electron diffraction, nano-beam electron diffraction, high resolution imaging and dark field electron holography. Ultramicroscopy, 2013, 131, 10-23.	1.9	115
58	Exploiting Lens Aberrations to Create Electron-Vortex Beams. Physical Review Letters, 2013, 111, 064801.	7.8	72
59	Towards rapid nanoscale measurement of strain in III-nitride heterostructures. Applied Physics Letters, 2013, 103, 231904.	3.3	7
60	Improved strain precision with high spatial resolution using nanobeam precession electron diffraction. Applied Physics Letters, 2013, 103, .	3.3	101
61	Mapping electronic reconstruction at the metal-insulator interface in LaVO <mml:math xmlns:mml="http://www.w3.org/1998/Math/MathML" display="inline"><mml:msub><mml:mrow /><mml:mn>3</mml:mn></mml:mrow </mml:msub>/SrVO<mml:math xmlns:mml="http://www.w3.org/1998/Math/MathML" display="inline"><mml:msub><mml:mrow< td=""><td>3.2</td><td>16</td></mml:mrow<></mml:msub></mml:math </mml:math 	3.2	16
62	Progress in electrons vortex creation and application in a transmission electron microscope. Microscopy and Microanalysis, 2013, 19, 1164-1165.	0.4	1
63	A holographic method to measure the source size broadening in STEM. Ultramicroscopy, 2012, 120, 35-40.	1.9	31
64	Strain mapping with nm-scale resolution for the silicon-on-insulator generation of semiconductor devices by advanced electron microscopy. Journal of Applied Physics, 2012, 112, .	2.5	16
65	Strain mapping for the silicon-on-insulator generation of semiconductor devices by high-angle annular dark field scanning electron transmission microscopy. Applied Physics Letters, 2012, 100, .	3.3	24
66	Depth strain profile with subâ€nm resolution in a thin silicon film using medium energy ion scattering. Physica Status Solidi (A) Applications and Materials Science, 2012, 209, 262-265.	1.8	4
67	A new way of producing electron vortex probes for STEM. Ultramicroscopy, 2012, 113, 83-87.	1.9	73
68	Field Mapping with Nanometer-Scale Resolution for the Next Generation of Electronic Devices. Nano Letters, 2011, 11, 4585-4590.	9.1	20
69	Strain measurement for the semiconductor industry with nm-scale resolution by dark field electron holography and nanobeam electron diffraction. , 2011, , .		2
70	Chemical Transformation of Au-Tipped CdS Nanorods into AuS/Cd Core/Shell Particles by Electron Beam Irradiation. Nano Letters, 2011, 11, 4555-4561.	9.1	33
71	Quantitative strain mapping of InAs/InP quantum dots with 1 nm spatial resolution using dark field electron holography. Applied Physics Letters, 2011, 99, .	3.3	30
72	Nano-field mapping for the semiconductor industry. Journal of Physics: Conference Series, 2011, 326, 012054.	0.4	1

#	Article	IF	CITATIONS
73	Strain measurement for the semiconductor industry with nm-scale resolution by dark field electron holography and nanobeam electron diffraction. Journal of Physics: Conference Series, 2011, 326, 012025.	0.4	2
74	Measuring two dimensional strain state of AlN quantum dots in GaN nanowires by nanobeam electron diffraction. Journal of Physics: Conference Series, 2011, 326, 012047.	0.4	4
75	Evaluation of the substitutional carbon content in annealed Si/SiGeC superlattices by dark-field electron holography. Journal of Physics: Conference Series, 2011, 326, 012024.	0.4	0
76	Measuring Strain in AlN/GaN Superlattices and Nanowires by NanoBeam Electron Diffraction. Microscopy and Microanalysis, 2011, 17, 1388-1389.	0.4	0
77	Dark field electron holography for strain measurement. Ultramicroscopy, 2011, 111, 227-238.	1.9	52
78	Field Mapping Of Semiconductors In A State-Of-The-Art Electron Microscope. AIP Conference Proceedings, 2011, , .	0.4	0
79	The reduction of the substitutional C content in annealed Si/SiGeC superlattices studied by dark-field electron holography. Semiconductor Science and Technology, 2011, 26, 125010.	2.0	11
80	Strain Measurement by Local Diffraction: NanoBeam Electron Diffraction (NBED) Compared to Convergent Beam (CBED) and Dark Holography. Microscopy and Microanalysis, 2011, 17, 1068-1069.	0.4	0
81	Annealed Siâ^•SiGeC Superlattices Studied by Dark-Field Electron Holography, ToF-SIMS and Infrared Spectroscopy. AIP Conference Proceedings, 2011, , .	0.4	0
82	Improved accuracy in nano beam electron diffraction. Journal of Physics: Conference Series, 2010, 209, 012063.	0.4	8
83	Strain evolution during the silicidation of nanometer-scale SiGe semiconductor devices studied by dark field electron holography. Applied Physics Letters, 2010, 96, 113508.	3.3	42
84	Strain mapping for the semiconductor industry by dark-field electron holography and nanobeam electron diffraction with nm resolution. Semiconductor Science and Technology, 2010, 25, 095012.	2.0	33
85	Dual Strained Channel co-integration into CMOS, RO and SRAM cells on FDSOI down to 17nm gate length. , 2010, , .		7
86	Improved precision in strain measurement using nanobeam electron diffraction. Applied Physics Letters, 2009, 95, .	3.3	144
87	Dark field electron holography for quantitative strain measurements with nanometer-scale spatial resolution. Applied Physics Letters, 2009, 95, .	3.3	52
88	A transition from local equilibrium to paraequilibrium kinetics for ferrite growth in Fe–C–Mn: A possible role of interfacial segregation. Acta Materialia, 2008, 56, 2203-2211.	7.9	69
89	Quantifying the Solute Drag Effect of Cr on Ferrite Growth Using Controlled Decarburization Experiments. Metallurgical and Materials Transactions A: Physical Metallurgy and Materials Science, 2007, 38, 2950-2955.	2.2	37